Decay of coupled plasmon - phonon modes in heavily doped semiconductors

1997 J. Phys.: Condens. Matter 9 4863

(http://iopscience.iop.org/0953-8984/9/23/010)

J. Phys.: Condens. Matter **9** (1997) 4863–4874. Printed in the UK PII: S0953-8984(97)81711-0

Decay of coupled plasmon–phonon modes in heavily doped semiconductors

A G Kozorezov, J K Wigmore and M Giltrow

School of Physics and Chemistry, Lancaster University, Lancaster LA1 4YB, UK

Received 10 February 1997

Abstract. For comparison with results obtained in recent phonon pulse experiments, we have calculated the relative magnitudes of different decay mechanisms for coupled plasmon–phonon modes in heavily doped GaAs. We find the dominant mechanism for energy loss by the coupled modes to be the direct excitation of bare phonons through second-order dipole moment and third-order anharmonic interactions, resulting in a lifetime of less than 1 ps for the particular material used in the experiments. Other mechanisms, notably lattice viscosity, electron–hole pair creation, rigorously forbidden at absolute zero, and the excitation of two electron–hole pairs, a higher-order effect but allowed at zero temperature, all give significantly smaller contributions to the decay rate. However, collision damping of the electrons through impurity scattering gives a lifetime which is much shorter than the above value, around 0.1 ps, but we note that this is an elastic scattering time, in contrast with the inelastic energy loss process. Linewidths in Raman scattering experiments yield the total scattering rate, which is dominated by the elastic process; currently only the phonon pulse measurements can give information directly on the inelastic process.

1. Introduction

It is well known that, in doped semiconductors in which the plasma frequency is close to the frequencies of polar optical phonons, neither plasmons (as long-wavelength elementary excitations of the ideal Fermi gas) nor polar optical phonons (as ideal lattice eigenstates) are elementary excitations of a crystal as a whole. In this situation, the strong interaction between them gives rise to the formation of coupled plasmon–phonon modes. These modes were first observed by Mooradian and Wright [1] in heavily doped GaAs using Raman scattering and have since been studied extensively [2–4]. Indeed, measurements of Raman spectra in heavily doped semiconductors and microstructures, especially those of reduced dimensionality, are often part of routine material characterization. The frequencies of the coupled modes, measured from the Stokes shift of the scattered light, give directly the carrier concentration, whilst the mobility of the carriers can be obtained from the line broadening.

Recently a new technique for studying coupled modes was demonstrated in which the acoustic phonons resulting from the decay of the modes were detected directly by superconducting bolometers [5]. In these experiments the coupled modes were excited by electrons tunnelling through a $GaAs/Al_xGa_{1-x}As$ double-barrier resonant tunnelling structure (DBRTS) into a heavily doped collector layer. The experiments confirmed for the first time that coupled-mode emission is the dominant mechanism for energy loss in such structures. Furthermore, the results also showed that the coupled modes themselves decayed by the emission of pure phonons, and not through electronic excitations. This was

0953-8984/97/234863+12$19.50

a surprising result since the data from Raman experiments imply that collision damping of the electron gas is the major source of line broadening. However, there have been no other experiments carried out directly on energy loss from coupled modes, nor any previous theoretical treatment of their decay. In this paper we consider all the possible mechanisms for the decay process and obtain numerical estimates for the samples used in [5]. We confirm that direct excitation of lattice vibrations is indeed the fastest inelastic process. However, we also find that this is an order of magnitude slower than (elastic) collision damping, which leads us therefore to the interesting question of the relation between energy dissipation and momentum redistribution of the plasmon collective mode of the Fermi gas. Specifically, is the overall phase coherence of the collective motion which forms the plasmon destroyed on the time scale of the elastic or the inelastic scattering processes?

We shall return to this important question after first developing the theory of the coupled mode scattering and decay processes, and comparing the numbers with experiment.

2. Interaction Hamiltonian

In this paper we follow the procedure of Hamiltonian diagonalization used by Peschke [6] and describe the bare plasmons by field operators after the model of Bohm and Pines. Then we add to the resulting Hamiltonian the phonon contribution and a term describing the interaction between bare plasmons and bare phonons. It is standard procedure also to keep the terms describing interactions between the electrons and plasmons, and between electrons and phonons. However, for our purposes it is sufficient to keep only the part of the Hamiltonian containing plasmon and phonon field operators. The resulting expression

$$H = \sum_{|\boldsymbol{q}|<q_c} \left[\overline{h}\Omega_{pl}(a_{\boldsymbol{q}}^{+}a_{\boldsymbol{q}} + \tfrac{1}{2}) - \mathrm{i}\sqrt{\frac{\overline{h}^2\Omega_{pl}\Omega_{LO}}{4}\,\frac{\varepsilon_0 - \varepsilon_\infty}{\varepsilon_0}}\,(a_{\boldsymbol{q}}^{+}b_{\boldsymbol{q}} - a_{\boldsymbol{q}}b_{\boldsymbol{q}}^{+} + a_{\boldsymbol{q}}b_{-\boldsymbol{q}} - a_{-\boldsymbol{q}}^{+}b_{\boldsymbol{q}}^{+}) \right] + \sum_{\boldsymbol{q}} \overline{h}\Omega_{LO}(b_{\boldsymbol{q}}^{+}b_{\boldsymbol{q}} + \tfrac{1}{2}) \tag{1}$$

describes the coupling between plasmon and phonon modes and will be taken as our unperturbed Hamiltonian. In (1), Ω_{pl} is the plasma frequency and Ω_{LO} the longitudinal polar optical frequency, $a_{\boldsymbol{q}}$ and $b_{\boldsymbol{q}}$ are the annihilation operators for bare plasmons and bare phonons, respectively, q_c is the cut-off wavevector of the plasmons, and ε_0 and ε_∞ are the static and optical dielectric constants, respectively, of the crystal.

To describe the mechanism of coupled-mode decay into lattice vibrational modes, we must add to this Hamiltonian the next-order terms in elastic displacements which describe the mode interactions. One mechanism for such an interaction is the anharmonic interaction which affects the elastic component of the coupled mode and eventually causes its decay. A second mechanism is that which couples crystal polarizability to lattice displacement. This type of interaction is governed by second-order elastic contributions to the crystal polarization [7]. Therefore we add to the interaction Hamiltonian terms describing the mode interactions via the third-order anharmonic potentials and second-order dipole moment.

We derive the required interaction Hamiltonian from the general form

$$H_{pl-ph} = \frac{1}{4\pi}\int \mathrm{d}\boldsymbol{r}\,\boldsymbol{D}'\cdot\boldsymbol{E}_{ph} \tag{2}$$

where $\boldsymbol{D}'$ is that part of electric displacement vector connected with plasma oscillations, given by

$$\boldsymbol{D}' = \varepsilon_\infty \boldsymbol{E}_{pl} = \mathrm{i}\sqrt{2\pi\varepsilon_\infty \overline{h}\Omega_{pl}} \sum_{|\boldsymbol{q}|<q_c} \frac{\boldsymbol{q}}{q} A_{\boldsymbol{q}} \exp(\mathrm{i}\boldsymbol{q}\cdot\boldsymbol{r}) \tag{3}$$

and $\boldsymbol{E}_{ph} = -4\pi\boldsymbol{P}$, where $\boldsymbol{P}$ is the polarization vector, and $A_{\boldsymbol{q}} \equiv a_{\boldsymbol{q}} + a^{+}_{-\boldsymbol{q}}$. The linear terms in the lattice polarization $\boldsymbol{P}$, when substituted into (1), result in coupling between plasmons and phonons. To account for the interaction between the coupled modes and vibrational excitations we keep the second-order terms in lattice polarization. In second quantization notation these terms result in the following interaction energy:

$$H^{(2)}_{pl-ph} = \frac{\mathrm{i}\bar{h}}{4M}\sqrt{\frac{2\pi\varepsilon_\infty \bar{h}\Omega_{pl}}{Na_0^3}} \sum_{\substack{\boldsymbol{q}',j';j'' \\ |\boldsymbol{q}|<q_c}} \frac{\mu^{(2)}(\boldsymbol{q};\boldsymbol{q}',j';-\boldsymbol{q}-\boldsymbol{q}',j'')}{\sqrt{\omega_{\boldsymbol{q}'j'}\omega_{-\boldsymbol{q}-\boldsymbol{q}'j''}}} A_{\boldsymbol{q}} B_{\boldsymbol{q}'j'} B_{-\boldsymbol{q}-\boldsymbol{q}'j''}. \tag{4}$$

Here $B_{\boldsymbol{q}} \equiv b_{\boldsymbol{q}} - b^{+}_{-\boldsymbol{q}}$, a_0^3 is the volume of the unit cell and M its mass, N is the number of cells in a crystal, and $\omega_{\boldsymbol{q}j}$ are the phonon frequencies for a phonon of branch j with wavevector $\boldsymbol{q}$. Also $\mu^{(2)}(\boldsymbol{q};\boldsymbol{q}',j';-\boldsymbol{q}-\boldsymbol{q}',j'') = \mu^{(2)}_{\alpha,\beta\gamma}(\boldsymbol{q};\boldsymbol{q}',j';-\boldsymbol{q}-\boldsymbol{q}',j'')(q_\alpha/q)e_\beta(\boldsymbol{q}',j')e_\gamma(-\boldsymbol{q}-\boldsymbol{q}',j'')$ is the effective value for the second-order dipole moment, and $e_\beta(\boldsymbol{q},j)$ the phonon unit polarization vector.

To account for phonon–phonon interactions we take the second-order dipole moment and third-order anharmonic terms [8–10]. Thus

$$\begin{aligned} H_{ph-ph} = {} & -\frac{\bar{h}}{4M}\sqrt{\frac{2\pi\bar{h}\Omega_{LO}}{Na_0^3}\left(\frac{1}{\varepsilon_\infty}-\frac{1}{\varepsilon_0}\right)} \\ & \times \sum_{\boldsymbol{q};\boldsymbol{q}',j';j''} \frac{\mu^{(2)}(\boldsymbol{q};\boldsymbol{q}',j';-\boldsymbol{q}-\boldsymbol{q}',j'')}{\sqrt{\omega_{\boldsymbol{q}',j'}\omega_{-\boldsymbol{q}-\boldsymbol{q}',j''}}} B_{\boldsymbol{q}} B_{\boldsymbol{q}',j'} B_{-\boldsymbol{q}-\boldsymbol{q}',j''} + \frac{1}{6\sqrt{N}}\left(\frac{\bar{h}}{2M}\right)^{3/2} \\ & \times \sum_{\boldsymbol{q}',j';\boldsymbol{q}'',j'';j'''} \frac{\Phi^{(3)}(\boldsymbol{q}',j';\boldsymbol{q}'',j'';-\boldsymbol{q}'-\boldsymbol{q}'',j''')}{\sqrt{\omega_{\boldsymbol{q}',j'}\omega_{\boldsymbol{q}'',j''}\omega_{-\boldsymbol{q}'-\boldsymbol{q}'',j'''}}} \\ & \times B_{\boldsymbol{q}',j'} B_{\boldsymbol{q}'',j''} B_{-\boldsymbol{q}'-\boldsymbol{q}'',j'''}. \end{aligned} \tag{5}$$

Here $\Phi^{(3)}(\boldsymbol{q}',j';\boldsymbol{q}'',j'';-\boldsymbol{q}'-\boldsymbol{q}'',j''') \equiv \Phi^{(3)}_{\alpha\beta\gamma}(\boldsymbol{q}',j';\boldsymbol{q}'',j'';-\boldsymbol{q}'-\boldsymbol{q}'',j''')e_\alpha(\boldsymbol{q}',j') \times e_\beta(\boldsymbol{q}'',j'')e_\gamma(-\boldsymbol{q}'-\boldsymbol{q}'',j''')$. In the coupled-mode representation the unperturbed plasmon–phonon Hamiltonian is diagonal. The interaction Hamiltonians (4) and (5) are derived using linear transformation of field operators:

$$\begin{pmatrix} a_{\boldsymbol{q}} \\ a^{+}_{-\boldsymbol{q}} \\ b_{\boldsymbol{q}} \\ b^{+}_{-\boldsymbol{q}} \end{pmatrix} = \begin{pmatrix} s_1 & t_1 & u_1 & v_1 \\ u_1^* & v_1^* & s_1^* & t_1^* \\ s_2 & t_2 & u_2 & v_2 \\ u_2^* & v_2^* & s_2^* & t_2^* \end{pmatrix} \begin{pmatrix} \alpha_{1,\boldsymbol{q}} \\ \alpha_{2,\boldsymbol{q}} \\ \alpha^{+}_{1,-\boldsymbol{q}} \\ \alpha^{+}_{2,-\boldsymbol{q}} \end{pmatrix}. \tag{6}$$

The elements of the transformation matrix (6) are the coordinates of the eigenvectors for the equation $[\alpha_{\boldsymbol{q}}, H] = E\alpha_{\boldsymbol{q}}$ [6]. They describe the relative contributions of plasma oscillations and lattice displacement to each coupled mode. The quantities $\alpha_{1,\boldsymbol{q}}$ and $\alpha_{2,\boldsymbol{q}}$ are the annihilation field operators for the coupled modes which we label by indices 1 and 2 for the upper (plasmon-like) and lower (phonon-like) coupled modes, respectively; thus $\Omega_1 > \Omega_2$, where $\Omega_{1,2}$ are the coupled-mode frequencies.

Labelling the decaying mode by $\boldsymbol{q}$ and after the above transformation keeping only those terms in the interaction Hamiltonian which describe the annihilation of an initial plasmon-like or phonon-like excitation at $\boldsymbol{q}$, and the creation of two phonons at $\boldsymbol{q}', j'$ and $\boldsymbol{q}-\boldsymbol{q}', j''$, we obtain with the use of (6):

$$H_{int1(2)} = \sum_{\boldsymbol{q}',j';j''} g_{1(2)}(\boldsymbol{q};-\boldsymbol{q}',j';-\boldsymbol{q}+\boldsymbol{q}',j'')\alpha_{1(2),\boldsymbol{q}} b^{+}_{\boldsymbol{q}',j'} b^{+}_{\boldsymbol{q}-\boldsymbol{q}',j''} \tag{7}$$

where

$$g_{1(2)}(\boldsymbol{q};-\boldsymbol{q}',j';-\boldsymbol{q}+\boldsymbol{q}',j'')=\frac{1}{\sqrt{\omega_{\boldsymbol{q}'j'}\omega_{\boldsymbol{q}-\boldsymbol{q}',j''}}}(\mathrm{i}\beta_{1(2)}C_{pl}+\gamma_{1(2)}C_{ph})_{j',j''} \quad (8)$$

with $\beta_1\equiv s_1+u_1^*$, $\beta_2\equiv t_1+v_1^*$, $\gamma_1\equiv s_2-u_2^*$, $\gamma_2\equiv t_2-v_2^*$,

$$\begin{aligned}(C_{pl})_{j',j''}&\equiv\frac{\hbar}{4M}\sqrt{\frac{2\pi\varepsilon_\infty\hbar\Omega_{pl}}{Na_0^3}}\mu^{(2)}_{j',j''},\\(C_{ph})_{j',j''}&\equiv\frac{1}{6\sqrt{N\Omega_{LO}}}\left(\frac{\hbar}{2M}\right)^{3/2}\tilde{\Phi}^{(3)}_{l,j',j''}.\end{aligned}\quad (9)$$

The subscripts refer to upper and lower modes, respectively. In (9) we dropped the wavevector dependence of the second-order dipole moment and cubic anharmonicity. In (9) also, $\tilde{\Phi}^{(3)}$ stands for the renormalized cubic anharmonicity arising from the contribution of the second-order dipole moment to three-phonon interactions. It can be seen from (7) that the second-order dipole moment contribution to the phonon–phonon interaction has the same form as the cubic anharmonic interaction. The modified potential for the cubic anharmonic interaction is

$$\tilde{\Phi}^{(3)}_{l,j',j''}=\Phi^{(3)}_{l,j',j''}-3\sqrt{\frac{4\pi M\Omega_{LO}^2}{a_0^3}\left(\frac{1}{\varepsilon_\infty}-\frac{1}{\varepsilon_0}\right)}\mu^{(2)}_{j',j''} \quad (10)$$

showing the relative strength of second-order dipole moment interactions relative to true cubic anharmonicity. According to [9, 10], $\mu^{(2)}>0$, while $\tilde{\Phi}^{(3)}<0$. Note that the final states are bare phonons. This follows immediately from energy and momentum conservation laws, which result in the strong inequality q', $|\boldsymbol{q}-\boldsymbol{q}'|\gg q_c>q$. Hence the decay products have such large wavevectors that the electron–phonon interaction is well beyond the cut-off and therefore does not modify the phonon properties in this part of Brillouin zone.

3. Coupled-mode decay rates

From (7)–(10) we can obtain the following expressions for the rates of spontaneous decay of the coupled modes into bare phonons:

$$\Gamma_1=\frac{2\pi}{\hbar^2}\sum_{\boldsymbol{q}',j',j''}\frac{|(\mathrm{i}\beta_1C_{pl}+\gamma_1C_{ph})_{j',j''}|^2}{\omega_{\boldsymbol{q}',j'}(\Omega_{1,\boldsymbol{q}}-\omega_{\boldsymbol{q}',j'})}\delta(\Omega_{1,\boldsymbol{q}}-\omega_{\boldsymbol{q}',j'}-\omega_{\boldsymbol{q}-\boldsymbol{q}',j''}) \quad (11a)$$

and

$$\Gamma_2=\frac{2\pi}{\hbar^2}\sum_{\boldsymbol{q}',j',j''}\frac{|(\mathrm{i}\beta_2C_{pl}+\gamma_2C_{ph})_{j',j''}|^2}{\omega_{\boldsymbol{q}',j'}(\Omega_{2,\boldsymbol{q}}-\omega_{\boldsymbol{q}',j'})}\delta(\Omega_{2,\boldsymbol{q}}-\omega_{\boldsymbol{q}',j'}-\omega_{\boldsymbol{q}-\boldsymbol{q}',j''}). \quad (11b)$$

It is seen from (11*a*) and (11*b*) that the coupled modes decay into phonons because of the coupling of the latter with both plasmon and phonon components, via the second-order dipole moment and third-order anharmonic potential, respectively. Thus, if for some reason the second-order dipole moment interaction is absent, then the upper mode can still decay via the crystal anharmonicity. The effective coupling constant for this process is weaker; the coefficient $C_{pl}\to 0$ and the weighting factor in (11*a*) take the form $|s_2-u_2^*|^2C_{ph}^2$, reflecting the contribution of anharmonicity to the plasmon-like decay rate. The physical meaning of this result is that the lattice viscosity relating to the phonon component of the coupled mode eventually kills the whole mode. The strength of this interaction can be related via the weighting factor to the amount of energy in the lattice component of the

coupled mode. Another situation is that in which the modes are weakly coupled so that the upper mode has only a small admixture of lattice distortion. Then $|s_1| \to 1$, $|t_1| \to 0$, and $|u_1| \to 0$, $|v_1| \to 0$, so that the decay of the upper mode is almost exclusively via the second-order dipole moment interaction with the coupling constant C_{pl}^2. Similarly, the decay of the lower mode is due almost totally to phonon–phonon interactions, although the coupling constant C_{ph}^2 has been renormalized, as shown in equation (9), to include the effects of the second-order dipole moment interaction on the effective three-phonon anharmonic interaction and on the phonon dispersion curve arising from the effects of screening. Thus $|t_2| \neq 0$, $|v_2| \neq 0$, $|v_2|/|t_2| = (\Omega_{LO} - \Omega_{TO})/(\Omega_{LO} + \Omega_{TO})$ and $|s_2| \to 0$, $|u_2| \to 0$.

Whilst discussing the interaction of coupled modes with phonons we have completely ignored the effects of screening on the effective coupling constants. To justify this procedure, we need to compare the screened Fröhlich scattering strength, $F_s^s(\Omega)$ with the unscreened Fröhlich scattering strength F_s^u. For small $q \ll q_c$ this ratio is $F_s^s(\Omega_{1(2)})/F_s^u = [\varepsilon_0/(\varepsilon_0 - \varepsilon_\infty)](\Omega_{1(2)}/\Omega_{LO})[(\Omega_{1(2)}^2 - \Omega_{TO}^2)/(\Omega_{1(2)}^2 - \Omega_{2(1)}^2)]$, where Ω_{TO} is the frequency of the transverse optical phonon [11]. For the lower coupled mode which is most affected by screening, this ratio in GaAs with $\hbar\Omega_1 = 50$ meV and $\hbar\Omega_2 = 30$ meV is $F_s^s(\Omega_2)/F_s^u \approx 0.63$. Therefore, even for the material with the strongest mode coupling (i.e. when Ω_1 and Ω_2 are at their closest), screening is not expected to cause significant modification to our estimates of the coupled-mode decay rates.

The general requirement for the vibrational decay of a coupled mode into two phonons to be allowed can be seen from (11) to be $\Omega_1 < 2\Omega_{max}$, where Ω_{max} is the maximum frequency across the whole phonon spectrum. If this condition is fulfilled, then the decay products are a pair of phonons with large and nearly opposite momenta to provide the conservation of a very small initial plasmon wavevector $q < q_c \ll \pi/a_0$. Thus a simple geometrical idea allows us to identify the possible decay channels. We must find, by inspection of the phonon dispersion curves, those values of the magnitude of the phonon wavevector for which the sum of the energies of a pair of corresponding phonons having opposite directions is equal to the energy of the initial coupled mode. We shall use this approach below to estimate the decay times for the 50 and 30 meV coupled modes in doped GaAs observed in [5].

4. Coupled-mode decay into two phonons in heavily doped GaAs

The maximum energy in the phonon spectrum of GaAs is 36.4 meV, corresponding to the LO phonon in the centre of the Brillouin zone. Therefore the two-phonon decay channel is allowed provided that the initial mode energy is below 72.8 meV. The corresponding electron density is $n^* = 2.7 \times 10^{18}$ cm^{-3}. Above this threshold, the two-phonon decay process is strictly prohibited. Having in mind the comparison with experiment [5], we performed a numerical evaluation of the decay rate for the particular case of plasmon-like mode energy $\hbar\Omega_1 = 50$ meV. There are in general five possible two-phonon decay channels allowed by the conservation laws.

Channel 1: Pl $\to$ LO + LA.
Channel 2: Pl $\to$ TO + LA.
Channel 3: Pl $\to$ LO + FT.
Channel 4: Pl $\to$ TO + FT.
Channel 5: Pl $\to$ LA + LA.

Here Pl refer to the upper coupled mode, LO to longitudinal optical phonons, and LA and FT to longitudinal acoustic and fast transverse acoustic phonons, respectively. Channels 3 and 4 involve phonons near the K point of the Brillouin zone; we assume these channels

to be allowed either at lower coupled mode energies, or through uncertainty in the mode energy due to its short lifetime.

The expression for the decay rate (equation (11*a*)) can be rewritten in a form showing the contribution of each channel:

$$\Gamma_1 = \frac{2\pi}{\hbar^2}\sum_{j',j''}|(\mathrm{i}\beta_1 C_{pl} + \gamma_1 C_{ph})_{j',j''}|^2 S_{j',j''} \tag{12}$$

where

$$S_{j',j''} = \sum_{\boldsymbol{q}'}\frac{\delta(\Omega_{1,\boldsymbol{q}} - \omega_{\boldsymbol{q}',j'} - \omega_{\boldsymbol{q}-\boldsymbol{q}',j''})}{\omega_{\boldsymbol{q}',j'}(\Omega_{1,\boldsymbol{q}} - \omega_{\boldsymbol{q}',j'})} \tag{13}$$

is the weighted two-phonon density of states for the nth decay channel. Assuming that dispersion curves for optical phonons in GaAs are horizontal lines across the whole Brillouin zone, it is straightforward to calculate weighted two-phonon density of states for all the decay channels. As a result, equation (12) acquires the following form:

$$\begin{aligned}\Gamma_1 = \frac{2}{\pi\hbar^2 v_l^3}\Bigg[&|(\mathrm{i}\beta_1 C_{pl} + \gamma_1 C_{ph})_{l,l}|^2\left(\frac{\Omega_1}{\Omega_{LO}} - 1\right) + 2|(\mathrm{i}\beta_1 C_{pl} + \gamma_1 C_{ph})_{l,t}|^2\left(\frac{\Omega_1}{\Omega_{TO}} - 1\right)\\ &+|(\mathrm{i}\beta_1 C_{pl} + \gamma_1 C_{ph})_{l,t}|^2\frac{\Omega_\nu^2}{\Omega_{LO}(\Omega_1 - \Omega_{LO})}\frac{\rho_{max}^{FT}}{\rho_{LA}(\Omega_\nu)}\\ &+2|(\mathrm{i}\beta_1 C_{pl} + \gamma_1 C_{ph})_{t,t}|^2\frac{\Omega_\nu^2}{\Omega_{TO}(\Omega_1 - \Omega_{TO})}\frac{\rho_{max}^{FT}}{\rho_{LA}(\Omega_\nu)}\\ &+2|(\mathrm{i}\beta_1 C_{pl} + \gamma_1 C_{ph})_{l,l}|^2\frac{\Omega_\nu^2}{\Omega_1^2}\frac{\rho_{LA}(\Omega_1/2)}{\rho_{LA}(\Omega_\nu)}\Bigg].\end{aligned} \tag{14}$$

Here for simplification we introduce $\Omega_\nu = 2\pi\nu$, where $\nu = 5$ THz is the frequency below which we may calculate phonon densities of states assuming a linear dispersion relation for longitudinal phonons. We use this quantity as a reference for phonon densities of states and take the ratios $\rho_{max}^{FT}/\rho_{LA}(\Omega_\nu)$ and $\rho_{LA}(\Omega_1/2)/\rho_{LA}(\Omega_\nu)$ from the results of known calculations (see, e.g., [12]). To carry out the numerical evaluation we now need to know C_{pl}, C_{ph}, β_1 and γ_1. The first quantity we calculate using the following values: $\mu_{t,t} = 0.177$; $\mu_{l,t} = 0.370$; $\mu_{l,l} = 0.605$ [9, 10]. From (9) we may then estimate $C_{ph}/C_{pl} = \frac{1}{6}(\tilde{\Phi}^{(3)}_{l,j',j''}/\mu^{(2)}_{j',j''})\sqrt{a_0^3}/\pi\varepsilon_\infty M\Omega_{LO}\Omega_{pl}$. Taking $|\tilde{\Phi}^{(3)}_{l,j',j''}| \approx 2\times 10^{13}$ erg cm^{-3} (according to [9, 10] $\tilde{\Phi}^{(3)}_{t,t,t} = -1.2\times 10^{13}$ erg cm^{-3}) and $\mu^{(2)} \approx 0.2$ esu cm^{-1} we come to the conclusion that $|C_{ph}/C_{pl}| \approx 0.06 \ll 1$. Therefore, even if the upper mode contains a significant lattice component, it is still true that $|\beta_1| \approx |\gamma_1|$ and $|\gamma_1 C_{ph}|/|\beta_1 C_{pl}| \ll 1$ so that to the accuracy of these estimates we may reasonably ignore the contribution of anharmonic effects to the decay of the plasmon-like mode.

Solving the eigenvalue problem $[\alpha_{\boldsymbol{q}}, H] = E\alpha_{\boldsymbol{q}}$ we find the following expressions:

$$\begin{aligned} s_1 &= \frac{1}{2}\frac{(\Omega_{pl} - \Omega_{LO})(\Omega_{pl} + \Omega_1)}{\Omega_1^2 - \Omega_2^2}\\ u_1 &= \frac{\Omega_{pl}}{\Omega_1}\frac{(\Omega_1 - \Omega_{pl})(\Omega_1 - \Omega_{LO})}{\Omega_1^2 - \Omega_2^2}\\ s_2 &= -\frac{\mathrm{i}}{2}\sqrt{\frac{\varepsilon_0}{\varepsilon_0 - \varepsilon_\infty}}\frac{\Omega_{pl}}{\Omega_1}\frac{\Omega_1^2 - \Omega_{LO}^2}{\Omega_1^2 - \Omega_2^2}\frac{\Omega_{LO}^2 - \Omega_2^2}{\Omega_{LO}\sqrt{\Omega_{LO}\Omega_{pl}}}\\ u_2 &= \frac{\mathrm{i}}{2}\sqrt{\frac{\varepsilon_0}{\varepsilon_0 - \varepsilon_\infty}}\frac{\Omega_{pl}}{\Omega_1}\frac{(\Omega_1 - \Omega_{LO})^2}{\Omega_1^2 - \Omega_2^2}\frac{\Omega_{LO}^2 - \Omega_2^2}{\Omega_{LO}\sqrt{\Omega_{LO}\Omega_{pl}}}. \end{aligned} \tag{15}$$

If we take the values $\hbar\Omega_1 = 52$ meV and $\hbar\Omega_2 = 31$ meV ($n = 1.25 \times 10^{18}$ cm^{-3}), then $s_1 \approx 0.35$, $u_1 \approx 0.03$, $s_2 \approx -0.22\mathrm{i}$ and $u_2 \approx 0.04\mathrm{i}$. Therefore, for the numerical evaluation we use $\beta_1 = 0.38$ and $\gamma_1 = -0.26\mathrm{i}$. Note that C_{ph} is negative so that the plasmon-like $\mathrm{i}\beta_1 C_{pl}$ and the phonon-like $\gamma_1 C_{ph}$ contributions to the coupling constant have the same sign, causing enhancement of the total coupling constant. Thus, if we neglect the anharmonic contribution, we shall obtain a lower limit for the decay rate. The ratio $|\gamma_1|/|\beta_1| \approx 0.7$, making the error due to disregarding the anharmonic contribution even less. Finally from (14) we arrive at the following numerical estimates for the two-phonon plasmon-like mode decay rate and lifetime, respectively: $\Gamma_1 \geqslant 1.1 \times 10^{12}$ s^{-1} and $\tau \leqslant 0.9$ ps. It should be noted that the decay is the result of a highly non-equilibrium situation. Hence the reverse process is insignificant, since the thermal population of the product phonons which might combine to create a coupled mode is negligibly small at low temperatures.

5. Other channels of coupled-mode decay

In this section we consider briefly other potential mechanisms for the decay of the plasmon-like mode. As summarized earlier, the main channels are as follows:

(i) lattice viscosity contributing to dielectric losses;

(ii) single-particle emission (Landau damping) which is strictly forbidden at zero temperature but is allowed in the exponential tail of the Fermi distribution at finite temperatures;

(iii) emission of two electron–hole pairs (here the term hole means a vacancy below Fermi level).

In addition, we estimate the following:

(iv) the magnitude of collisional damping in this system.

(i) The effect of lattice viscosity may be described phenomenologically by the following contribution to the imaginary part of the total dielectric function [4]:

$$\varepsilon_L'' = \varepsilon_\infty \frac{\Omega_{LO}^2 - \Omega_{TO}^2}{(\Omega_{TO}^2 - \Omega^2)^2}\Omega\gamma_L \tag{16}$$

where, for GaAs, $\gamma_L = 0.248$ meV. Thus, $\varepsilon_L''(\Omega_1) = 0.016$ and $\tau_L \approx 15$ ps. Note that this effect is totally different from the anharmonic damping of the lattice component of the coupled mode discussed above.

(ii) We estimate the magnitude of creation of single electron–hole pairs using the Lindhard dielectric function ($f(E_k)$ is the Fermi–Dirac distribution function):

$$\varepsilon''(\boldsymbol{q}, \omega) = -\frac{4\pi e^2}{q^2}\,\mathrm{Im}\left(\sum_{\boldsymbol{k}} \frac{f(E_{\boldsymbol{k}+\boldsymbol{q}}) - f(E_{\boldsymbol{k}})}{E_{\boldsymbol{k}+\boldsymbol{q}} - E_{\boldsymbol{k}} - \hbar\omega - \mathrm{i}0}\right). \tag{17}$$

For the case of a degenerate semiconductor this gives

$$\varepsilon_L''(\Omega_{pl}) \approx \frac{e^2 k_F}{2\varepsilon_F}\frac{k_B T}{\varepsilon_F}\frac{1}{x^3}\exp\left\{-\frac{\varepsilon_F}{k_B T}\left[\left(\frac{\hbar\Omega_{pl} - \varepsilon_F x^2}{2\varepsilon_F x}\right)^2 - 1\right]\right\}$$

where $x = q/k_F$. Here ε_F and k_F are the Fermi energy and momentum, respectively. For $x = 0.35$ and $T_e \approx 20$ K we obtain $\varepsilon_L''(\Omega_p) \approx 1 \times 10^{-3}$ and correspondingly $\tau_{LD} \approx 0.25$ ns, which is much longer than for other processes discussed so far. This is a consequence of the fact that we are considering plasmon-like mode decay into electron–hole pairs for plasmons

having small values of the parameter x. Therefore, in spite of the finite temperature, the plasmon is well below the threshold for Landau damping, and the only allowed single-particle interactions with small momentum transfer are in the exponential tail of the Fermi distribution. However, this estimate is only an approximation as elastic scattering present in the electron gas may significantly modify the form of the dielectric function.

(iii) In contrast with the above, coupled-mode decay into two electron–hole pairs, which proceeds via higher-order perturbation processes in the ideal electron gas, is allowed by the conservation laws even at zero temperature. This process is believed to be the major mechanism for plasmon decay in metals, and in order to estimate its magnitude we borrow directly the expression for the decay rate with a screened interaction [14]:

$$\Gamma_{pr-pr} = \frac{4}{5\pi}\Omega_{pl}N(\Omega_{pl})x^2\left(\frac{\Omega_{pl}}{2\varepsilon_F}\right)^2 \tag{18}$$

where $N(\Omega_{pl})$ is the screening factor. For $x = 0.3$ we can obtain $\tau_{pr-pr} \geqslant 5$ ps. In order to extend this result to describe plasmons in a heavily doped semiconductor, it is necessary to add an extra term due to lattice polarizability to the total dielectric function, in addition to the contribution from electron polarizability. The screening factor $N(\Omega_{pl})$ contains the squared modulus of the total dielectric function in the denominator [14], and therefore we would expect a reduction in $N(\Omega_{pl})$ and corresponding increase in τ_{pr-pr}, so that the value of 5 ps is a lower limit. Elastic scattering in the electron gas is less important in this case since the basic process is allowed even at absolute zero.

(iv) Finally we estimate the magnitude of the lifetime due to collisional damping in the Fermi gas. The expression for the scattering rate of the coupled modes due to this process may be written in the form $\Gamma_{1,coll} = (\Omega_1/2)[\varepsilon_c''(q,\Omega_1)/\varepsilon''(q,\Omega_1)]$, where $\varepsilon_c''(q,\Omega_1)$ is the critical value of the imaginary part of the dielectric function for which the plasmon ceases to exist, i.e. when the lifetime of the coupled mode is shorter than collision time and $\varepsilon''(q,\Omega_1)$ is the Lindhard–Mermin dielectric function. The value of $\varepsilon_c''(q,\Omega_1)$ has been calculated in [6], facilitating our estimate. A typical value of the mobility in GaAs in the range of carrier concentrations around 10^{18} cm^{-3} is (2–3) $\times$ 10^3 cm^2 V^{-1} s^{-1} which gives the transport relaxation time in the range $\tau_{tr} \approx 0.1$–0.15 ps. It can be shown from the Lindhard–Mermin dielectric function that the coupled-mode lifetime with respect to collisional damping is $\tau_{coll} \geqslant \tau_{tr}$ so that $\tau_{coll} \geqslant 0.1$–$0.15$ ps. This estimate agrees well with the experimental value derived from the measurements of the Stokes linewidth in Raman spectra [3, 4]. This is not surprising since in the Raman scattering geometry the transferred momentum is fixed, and therefore the linewidth should reflect the uncertainty in plasmon momentum [2].

Summarizing the results of our numerical estimates we arrive at the following hierarchy of the plasmon–phonon lifetimes:

$$\tau_{coll} \ll \tau \ll \min\{\tau_{LD}, \tau_L, \tau_{pr-pr}\}. \tag{19}$$

6. Discussion of the experimental evidence

Even with allowance for the appreciable uncertainty attached to some of the values used, our calculations suggest clearly that the dominant mechanism for coupled-mode energy loss at low temperatures is direct excitation of lattice vibrations, and not electronic processes. The decay rate for phonon emission is at least an order of magnitude larger than that due to lattice viscosity or the creation of electron–hole pairs. To our knowledge the only experimental data relating to this situation are Raman linewidth measurements, widely used

for many years [2], and our own direct observations using phonon pulse techniques of the coupled-mode decay products [5]. However, the Raman linewidths reflect the uncertainty in a single component of the quasi-momentum of the coupled mode, which includes both elastic and inelastic processes. Ramsteiner *et al* [3] found that their measured linewidths correlated with the mobility of the sample, which was dominated by the elastic collisions with impurities. As we saw earlier, collision damping is several times faster than energy loss by phonon excitation. However, it does not give rise to coupled-mode decay, only to randomization of momentum. Hence the Raman experiments do not give information directly on energy loss processes for coupled modes. Similarly, transport measurements on an electron gas invariably yield the elastic scattering time and not the time for inelastic energy loss.

In contrast, the phonon pulse experiments give information relating directly to the energy loss mechanism and indeed are insensitive to elastic scattering. Details of the technique can be found in [5]. The coupled modes were excited in the collector region of a DBRTS, consisting of GaAs doped nominally with silicon (2×10^{18} cm^{-3}). Tunnelling electrons could be injected into the collector with various energies, and the resulting acoustic phonons detected via an array of superconducting aluminium bolometers on the opposite polished face of the wafer. The DBRTS devices and bolometers were 65 μm in size and the pulses 10 ns long so that high temporal and spatial resolution could be achieved, and LA and transverse acoustic (TA) polarizations resolved in any direction. By observing the dependence of the detected phonon flux for different phonon polarizations as a function of electron energy it was possible to identify the mechanisms of energy loss and to arrive at the conclusion that coupled modes decayed predominantly via lattice excitations, as will now be explained.

Figure 1 shows the relevant data, which have been normalized to the tunnelling current, so that the displayed quantity is the phonon flux per electron. The results for two samples with different doping densities and hence carrier concentrations are shown, but the basic features described below have been confirmed for many DBRTS devices. It is seen that the TA mode has an approximately linear dependence on electron energy, whilst the LA mode is essentially independent of electron energy. The results can be understood by the following model of electron energy loss, summarized in figure 2. An injected electron initially loses energy by emitting a cascade of coupled modes, plasmon like at 50 meV and phonon like at 30 meV [12], until the energy has fallen to a level below the threshold for the phonon-like mode. This process is an order of magnitude stronger than single-particle electron–electron scattering. The coupled modes decay into high-frequency phonons which subsequently suffer anharmonic down-conversion resulting in TA ballistic phonons [13], so that the TA flux per electron at the bolometer scales with initial electron energy, less 30 meV. Fine structure on the TA mode variation confirmed the cascade mechanism and also gave the values of the coupled-mode energies. It should be noted that the observation of structure relating to the energies of the coupled modes also confirmed that the coupled modes did not thermalize amongst themselves but decayed spontaneously before any thermalizing collisions could take place. It is easy to confirm by a simple calculation that this result is reasonable. From the bias voltage (300 mV), current density (5 mA) and collector volume (65 μm $\times$ 65 μm $\times$ 0.5 μm) an average separation of 0.1 μm between coupled modes could be inferred, which is an order of magnitude larger than the distance travelled in the coupled-mode lifetime, 1 ps.

Below 30 meV, electrons can lose further energy only through single-particle collisions, with the resultant heating of the Fermi gas. Thus, as the bias voltage is varied, the relative amounts of energy lost into the two channels, coupled-mode emission and single-particle excitation, fluctuate but with a maximum of 30 meV available for heating the Fermi gas,

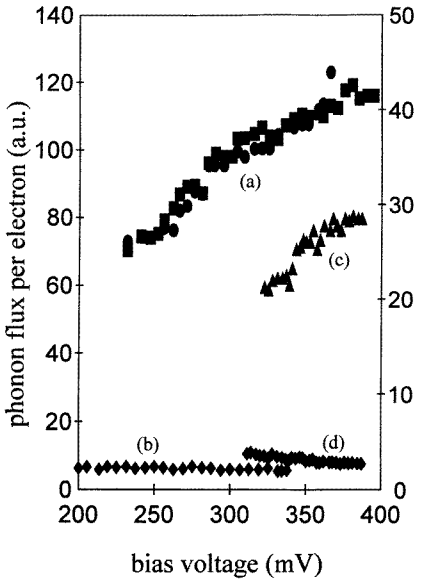

Figure 1. Dependence of the ballistic phonon fluxes measured at the bolometer as a function of initial electron energy for two different carrier concentrations: (a) TA phonons; (b) LA phonons for a carrier concentration pf 2×10^{18} cm^{-3}; (c) TA phonons; (d) LA phonons for a carrier concentration of 1×10^{18} cm^{-3}. The data are normalized to the tunnelling current, and hence to the number of electrons participating in the energy loss process. The LA and TA phonons can be distinguished through their different arrival times. Note the different relative magnitudes for the different plasma energies.

regardless of the incident energy. We were able to calculate the temperature to which the Fermi gas was heated by this process using the expression for the power input P per electron:

$$P = \sum_{m=1}^{\infty} \left\{ \frac{0.256}{m^5} T_e^5 \gamma \left[5; \frac{25.7m}{T_e} \right] + \frac{0.072}{m^3} T_e^3 \gamma \left[3; \frac{25.7m}{T_e} \right] \right\} \text{ eV s}^{-1}. \quad (20)$$

Here $\gamma(n; \alpha)$ is an incomplete gamma function. We derived this formula having transformed the expressions given by Kogan [15] into series expansions based on the solution for the degenerate limit. At the resonant tunnelling peak, $P = 4.5 \times 10^5$ eV s^{-1}, yielding a maximum value for T_e of 22 K.

At this temperature the Fermi gas is well below the threshold for optical phonon emission, and loses energy by radiating acoustic phonons, predominantly longitudinal, via deformation potential and piezoelectric coupling. We can therefore regard the detected LA phonon flux per electron as a direct indicator of that component of the original electron energy that is dissipated by single-particle processes, since these alone result in heating of the Fermi gas. The fact that it is independent of the injected electron energy confirms that only the residual 30 meV, below the excitation threshold for the phonon-like mode, gave rise to heating of the Fermi gas. Thus we can infer that the majority of the incident energy, which went into coupled-mode excitation, did not finish up in the Fermi gas but as down-converted TA phonons. Hence we conclude that the coupled modes decay by lattice, and not by electronic excitations.

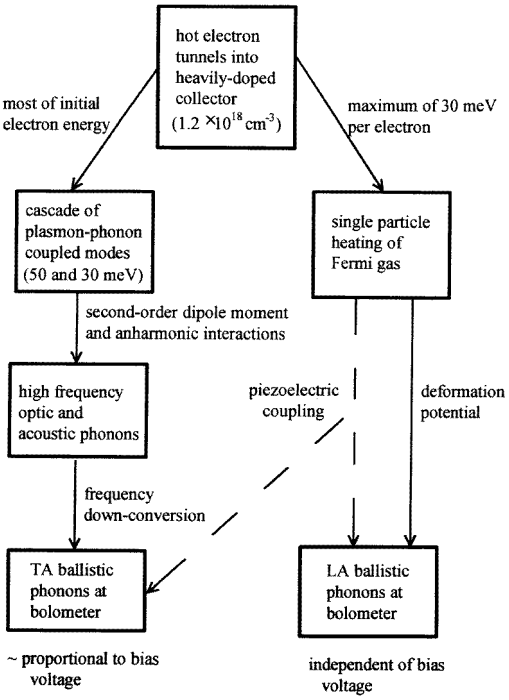

Figure 2. Summary of the energy conversion processes, from the initial kinetic energy of the tunnelling electron, to the final LA and TA phonons arriving at the bolometer.

7. Conclusions

Our results, both theoretical and experimental, have shown that energy loss by plasmon–phonon coupled modes occurs predominantly via emission of phonons, and not through electronic excitations. Furthermore, we found that decay takes place on a significantly longer time scale than that of collision damping. However, the latter process is elastic so that, although the momenta of the individual electrons are changed by scattering, the overall phase coherence between electron wavefunctions is maintained. Thus the correlated motion that constitutes plasmon behaviour is unaffected by collision damping.

Acknowledgment

We are grateful to the Engineering and Physical Sciences Research Council for supporting both the work and the personnel (MG and AK).

References

[1] Mooradian A and Wright G B 1966 *Phys. Rev. Lett.* **16** 999
[2] Abstreiter G, Cardona M and Pinczuk A 1984 *Light Scattering in Solids* vol 4, ed M Cardona and G Guntherodt (Berlin: Springer) p 5
[3] Ramsteiner M, Wagner J, Hiesinger P and Kohler K 1993 *J. Appl. Phys.* **73** 5023
[4] Nowak U, Richter W and Sachs G 1981 *Phys. Status Solidi* (b) **108** 131

[5] Giltrow M, Kozorezov A, Sahraoui-Tahar M, Wigmore J K, Davies J H, Vogel B, Stanley C R and Wilkinson C D W 1995 *Phys. Rev. Lett.* **75** 1827
[6] Peschke C 1993 *J. Appl. Phys.* **74** 327
[7] Born M and Huang K 1954 *Dynamical Theory of Crystal Lattices* (Oxford: Oxford University Press)
[8] Ferry D C 1974 *Phys. Rev.* B **10** 4277
[9] Flytzanis C 1972 *Phys. Rev. Lett.* **29** 772
[10] Flytzanis C 1972 *Phys. Rev.* B **6** 1264
[11] Kim M E, Das A and Senturia S D 1978 *Phys. Rev.* B **18** 6890
[12] Rorison J M and Herbert D C 1986 *J. Phys. C: Solid State Phys.* **19** 399
Rorison J M and Herbert D C 1986 *J. Phys. C: Solid State Phys.* **19** 6357
[13] Tamura S 1984 *Phys. Rev.* B **30** 849
[14] DuBois D F and Kivelson M G 1969 *Phys. Rev.* **186** 409
[15] Kogan S M 1963 *Sov. Phys.–Solid State* **4** 1813